

## **ESI: Towards understanding the catalytic properties of lead-based ballistic modifiers in double base propellants**

*Lisette R. Warren, Colin R. Pulham, and Carole A. Morrison\**

*EaSTCHEM School of Chemistry, University of Edinburgh, The King's Buildings, David Brewster Road, Edinburgh, EH9 3FJ, UK.*

### **Supplementary information**

#### Contents

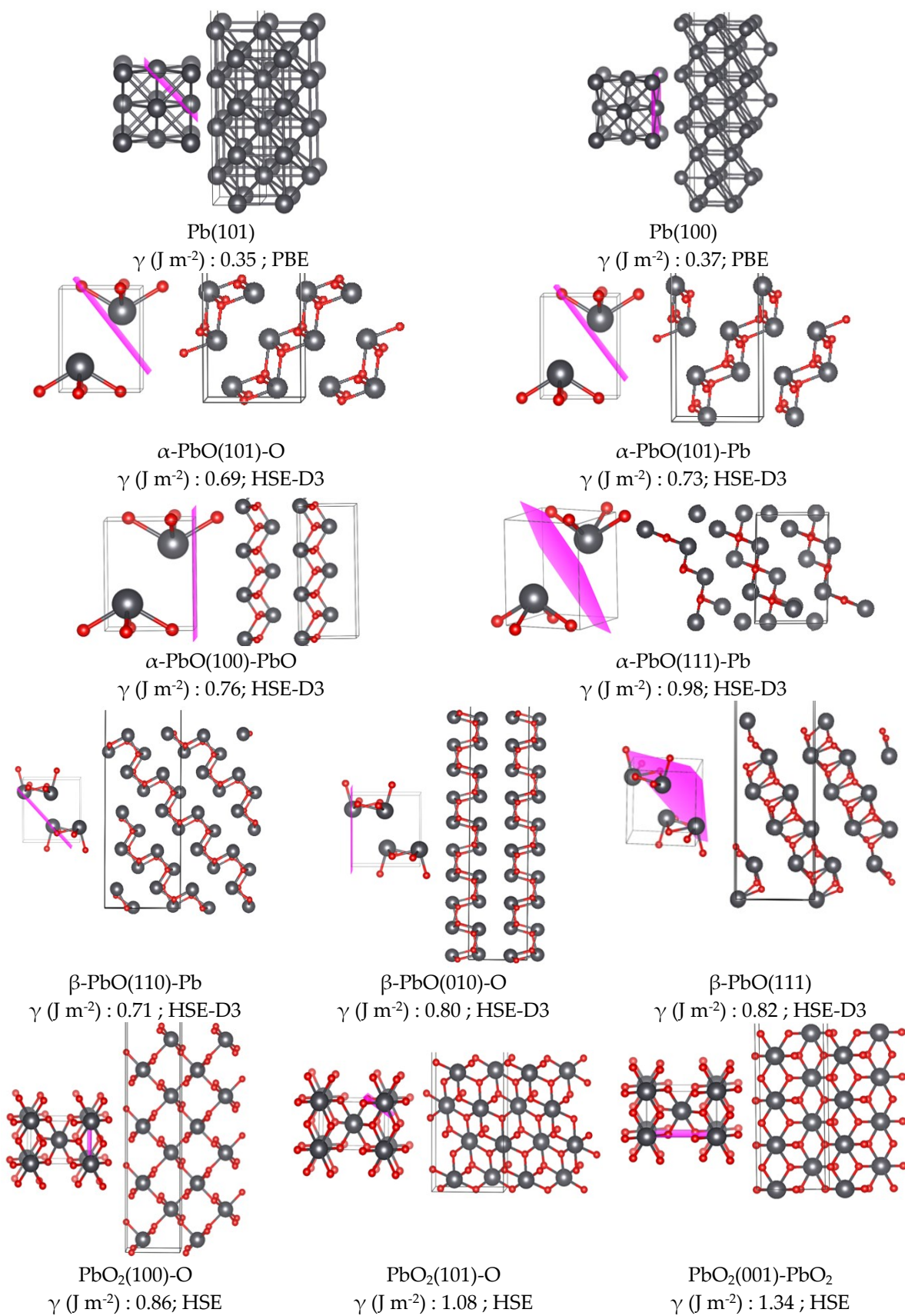
<b>S1 Structural and electronic data for optimisation of bulk systems .....</b>	<b>2</b>
<b>S2 Composition of other (less stable) studied surfaces and surface energies .....</b>	<b>3</b>
<b>S3 Convergence of surface energy and surface work function with respect to the number of layers in the model .....</b>	<b>5</b>
<b>S4 Electronic density of states of most stable surface .....</b>	<b>6</b>
<b>S5 Surface calculations .....</b>	<b>7</b>
<b>S6 Initial and optimised adsorption models for carbon binding study .....</b>	<b>7</b>
<b>References .....</b>	<b>14</b>

## S1 Structural and electronic data for optimisation of bulk systems

**Table S1.** Crystal and electronic structure data for all bulk systems calculated using various functionals. (AO) stands for atom-only optimisation.  
All calculations performed with CRYSTAL17.

Parameter	Functional	a (Å)	b (Å)	c (Å)	$\beta$ (°)	Volume (Å <sup>3</sup> )	Band gap (eV)
Pb	Experiment	4.95	4.95	4.95	90	121.29	Metal
	PBE-D3	4.98	-	-	-	123.80	Metal
	HSE06-D3	4.90	-	-	-	120.94	Metal
$\alpha$ -PbO	Experiment	3.96	3.96	5.01	90	78.56	1.9
	PBE-D3	4.07	-	4.96	-	82.28	1.24
	PBE0-D3	3.99	-	4.93	-	78.43	2.47
	B3LYP-D3	4.04	-	4.88	-	79.73	2.37
	HSE06-D3	3.99	-	4.87	-	77.43	1.72
	HSE06	4.03	-	4.68	-	79.32	1.98
	HSE06-D3 (AO)	3.96	-	5.01	-	78.56	1.78
$\beta$ -PbO	Experiment	5.90	5.49	4.75	90	153.96	2.6, 2.7
	PBE-D3	5.87	5.42	4.87	-	155.03	1.85
	PBE0-D3	5.80	5.41	4.74	-	148.73	3.40
	B3LYP-D3	5.79	5.37	4.75	-	147.68	3.25
	HSE06-D3	5.79	5.39	4.74	-	147.87	2.82
	HSE06	6.25	5.69	4.77	-	169.51	3.06
	HSE06-D3 (AO)	5.90	5.49	4.75	90	153.96	2.89
$\beta$ -PbO <sub>2</sub>	Experiment	4.96	4.96	3.39	90	83.27	0.61
	PBE-D3	5.06	-	3.48	-	89.16	0.02
	PBE0-D3	4.95	-	3.39	-	83.15	0.51
	B3LYP-D3	4.98	-	0.69	-	85.12	0.004
	HSE06-D3	4.95	-	3.39	-	83.26	0.13
	HSE06	5.00	-	3.40	-	85.12	0.09
$\alpha$ -Bi <sub>2</sub> O <sub>3</sub>	Experiment	5.85	8.17	7.51	113	330.15	2.5, 2.8 <sup>6,7</sup>
	PBE	6.02	8.23	7.50	111.87	344.91	2.14
	PBE0	5.94	8.12	7.46	112.32	332.85	3.89
	B3LYP	6.03	8.34	7.57	112.46	351.83	3.66
	HSE06	5.94	8.14	7.46	112.24	333.85	3.23
	HSE06-D3	5.89	7.93	7.36	112.01	318.70	3.15
SnO <sub>2</sub>	Experiment	4.74	4.74	3.19	90	71.53	3.56
	PBE-D3	4.82	-	3.26	-	75.76	0.51
	PBE0-D3	4.75	-	3.20	-	72.18	3.39
	B3LYP-D3	4.77	-	3.23	-	73.38	2.70
	HSE06-D3	4.75	-	3.20	-	72.21	2.78
	HSE06	4.78	-	3.21	-	73.48	2.59

## S2 Composition of other (less stable) studied surfaces and surface energies



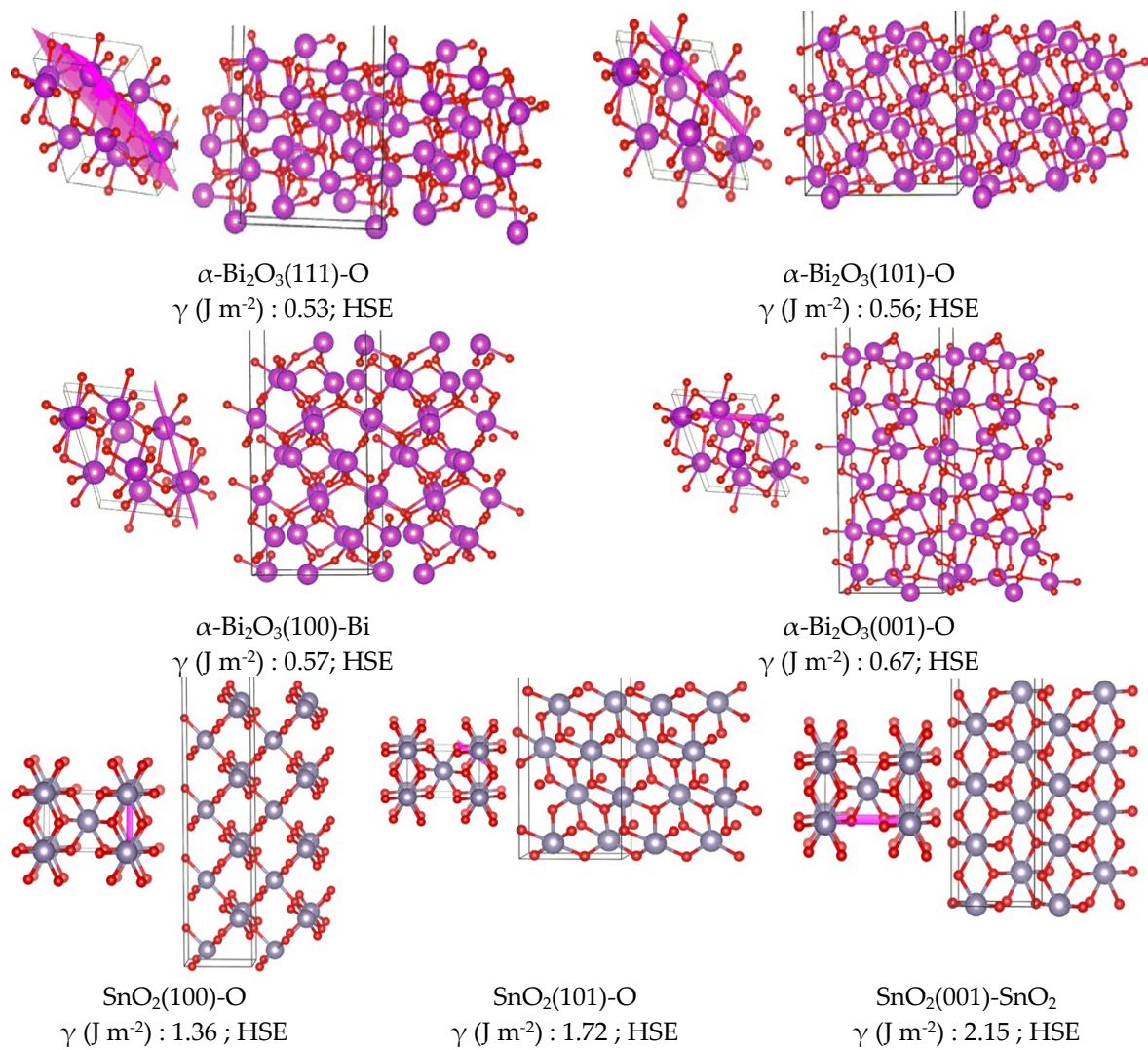


**Figure S1.** Ball-and-stick models of studied low index Miller surfaces.

Surfaces are 2D periodic models, with no directionality along z-direction.

$\gamma$  represents relaxed surface energies; HSE the hybrid HSE06 functional; -D3 the application of Grimme D3 dispersion correction.

### S3 Convergence of surface energy and surface work function with respect to the number of layers in the model

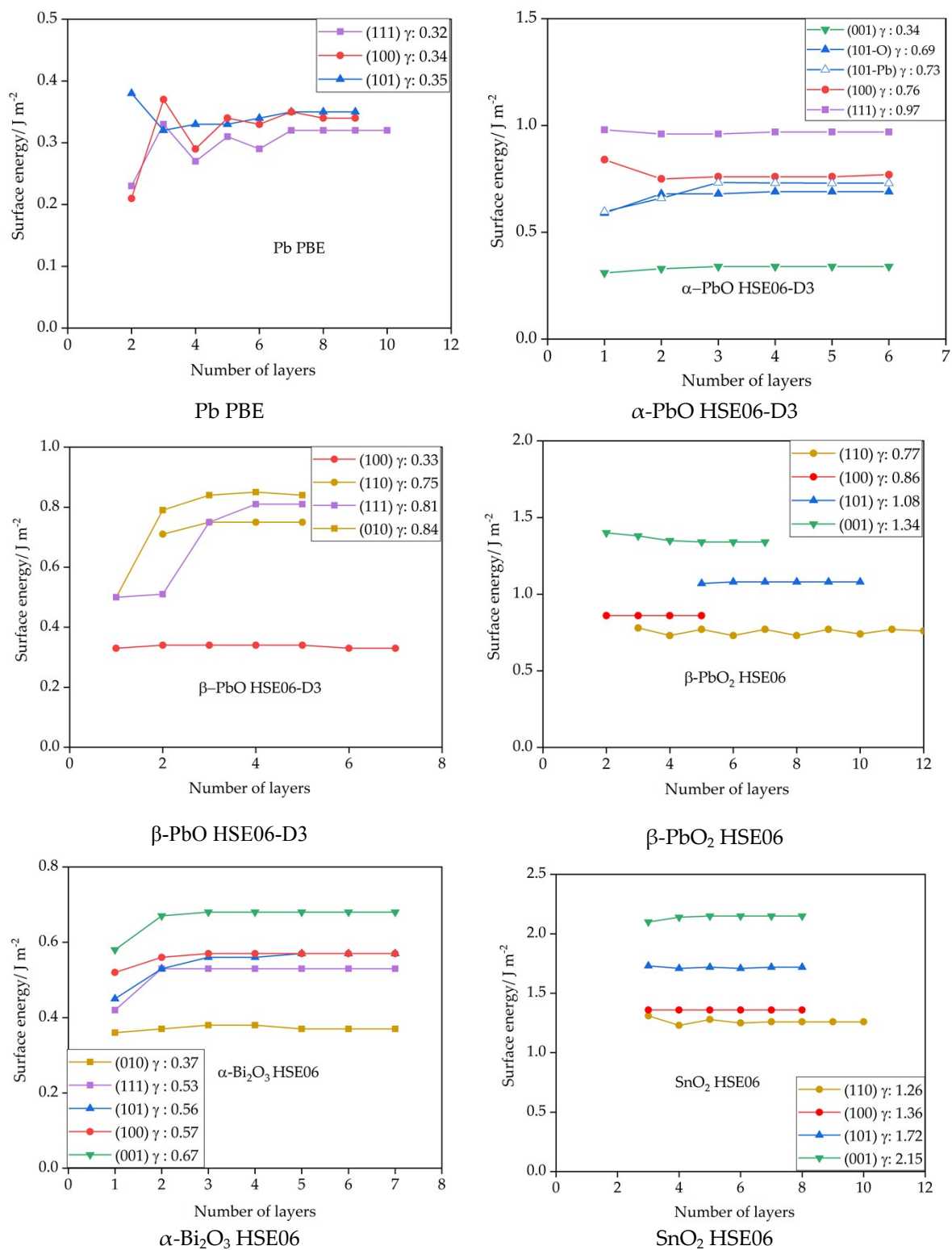


**Figure S2.** Convergence of surface energies with number of layers for each studied surface of the six systems.

## S4 Electronic density of states of most stable surface

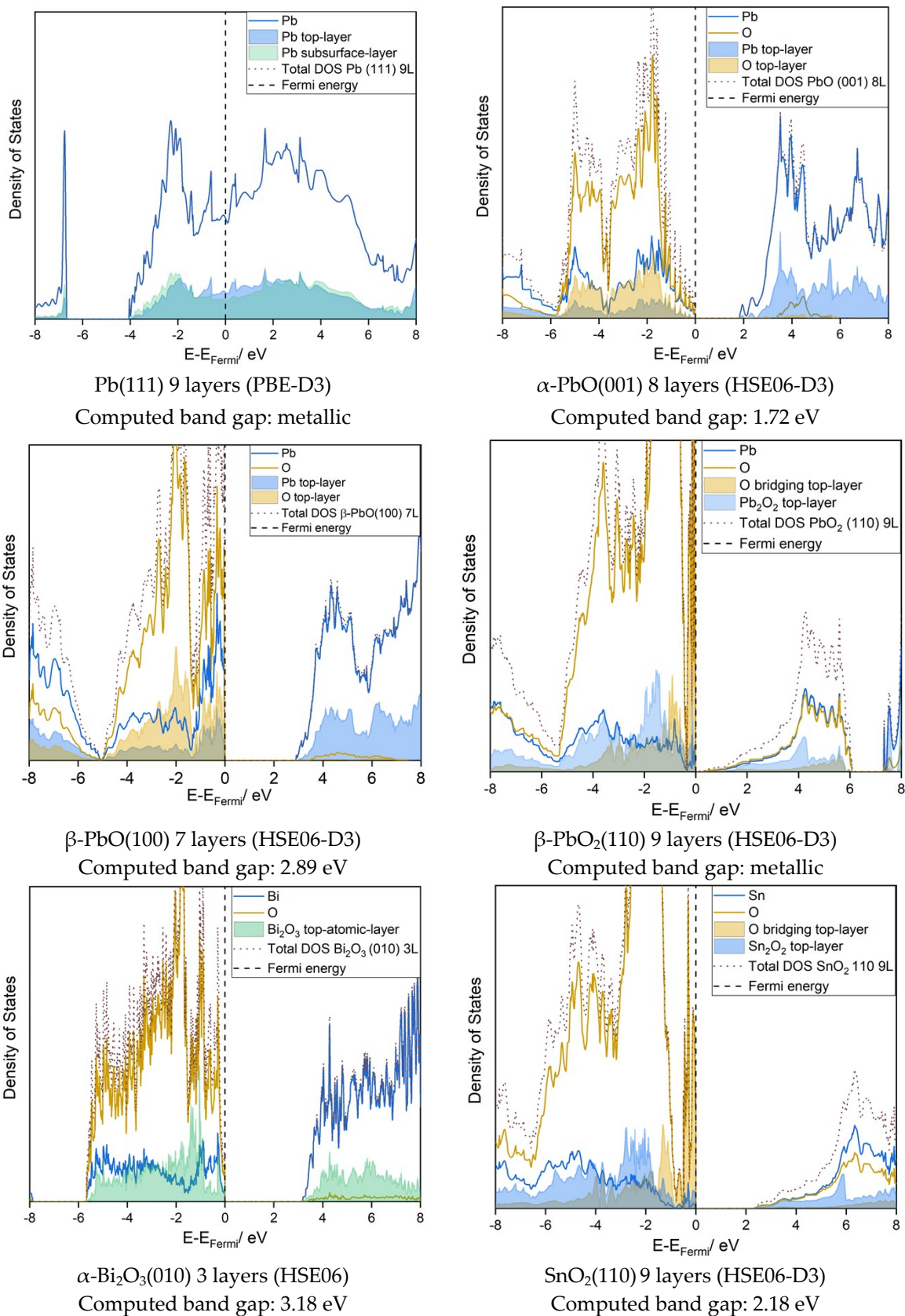


**Figure S3.** Computed density of states for the best fitting functional for each of the six studied systems.

## S5 Surface calculations

**Surface energy calculations:** Within the slab model approach, the general equation for surface energy is defined:

$$\gamma = \frac{\Delta E_{surf}^n}{2A} = \frac{(E^n - nE_{bulk})}{2A}$$

Where  $E^n$  is the energy of an  $n$ -layer slab,  $n$  is the number of bulk units.  $E_{bulk}$  is the energy of a single layer of bulk material, and  $A$  is the surface area of the slab.  $\Delta E_{surf}^n$  is the energy per unit area required to form the surface from the bulk. The factor  $\frac{1}{2}$  accounts for the existence of two limiting surfaces, thus the two surfaces in the slab model should be identical to calculate the surface energy. For sufficiently large values of  $n$ , the surface energy is expected to converge with respect to the number of atomic layers.

**Surface work function calculations:** Computationally the surface work function is defined as:

$$\phi = -e\Phi - E_F$$

From a density functional calculation perspective, calculations are performed on a 2D surface, which is infinite along the  $x$ - and  $y$ - directions, and with a finite vacuum thickness along the  $z$ -axis. Thus to estimate the surface work function, knowledge of the electrostatic potential in the vacuum and the Fermi energy is required.

Within CRYSTAL, the zero of the electrostatic potential is defined such that  $\Phi(\infty) = -\Phi(-\infty)$ , and for clean unrelaxed surfaces (symmetric), the electrostatic potential  $\Phi$  is zero. Thus, the work function is simply  $-E_F$ , which is determined by the number of electrons in the system. In this work the slabs were modelled with enough thickness that the Fermi energy did not change with increasing numbers of layers.

**Carbon adsorption energy calculations:** After the most stable surface was deduced for the bare surface models, a continuous layer of amorphous carbon has been built within the periodic boundary condition constraints using Materials Studio. The interaction between the carbon layer and the bare surface was studied via the calculated adsorption energy, determined by the following equation:

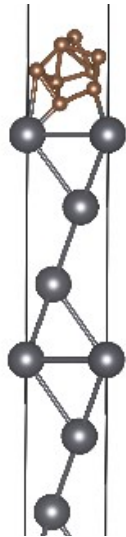
$$E_{ads} = E_{C|surf} - E_{surf}E_C$$

Where  $E_{ads}$  is the adsorption energy,  $E_{C|surf}$  is the total energy of the optimised carbon layer on the surface, and  $E_{surf}E_C$  is a single point energy value, obtained by shifting the optimised carbon layer from the bare surface along the  $c$ -axis. To allow this, a vacuum of 20 Å has been used in the models.

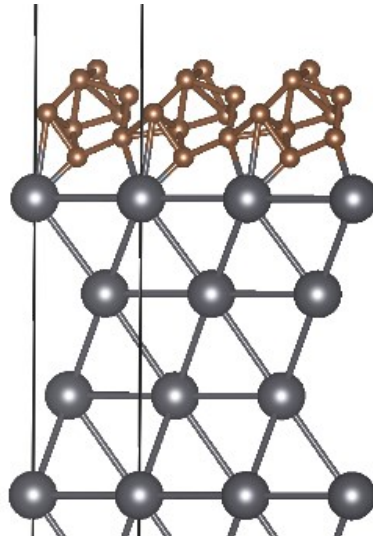
## S6 Initial and optimised adsorption models for carbon binding study

Initial adsorption models for binding of amorphous carbon to each surface are shown below in Figure S4. In order to initially adsorb a similar amount of carbon to the surface, each model has approx. 1 carbon atom per 1.4 Å<sup>2</sup> of surface area. Initial surface oxygen-carbon distances are set to about 1.3-1.5 Å, and for surface metal-carbon bonds, distances are about 1.7-1.8 Å.

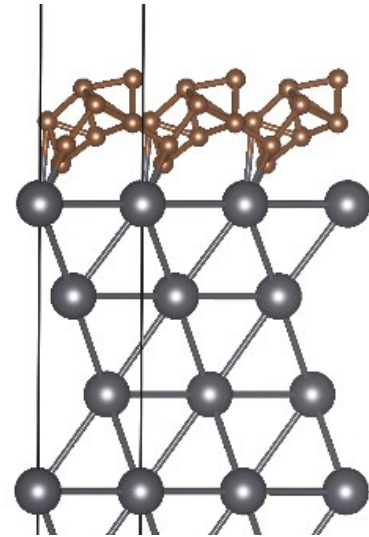




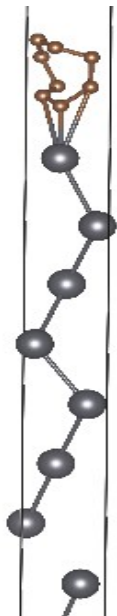
Initial carbon binding model to Pb(111) 10L



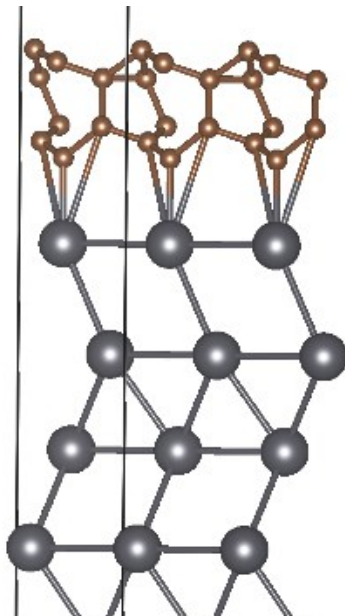
Initial binding to Pb(111) 10L 3 x 1 x 1 for visualisation



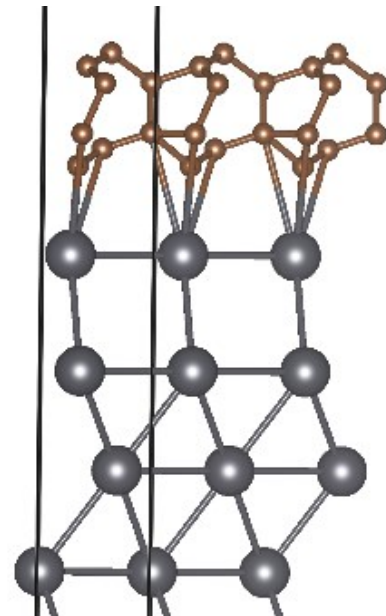
Initial binding to Pb(111) 10L 1 x 3 x 1 for visualisation



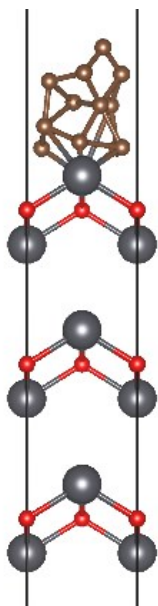
Optimised carbon binding model to Pb(111) 10L



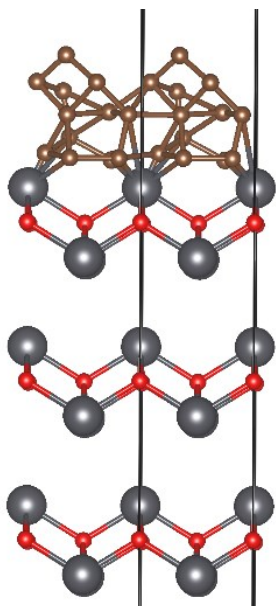
Optimised binding to Pb(111) 10L 3 x 1 x 1 for visualisation



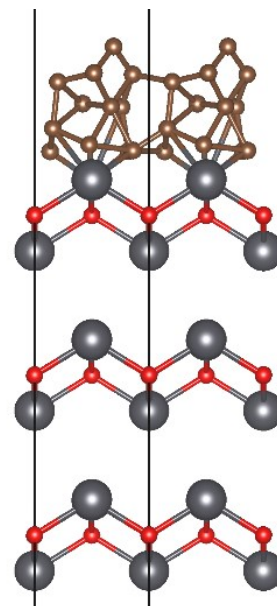
Optimised binding to Pb(111) 10L 1 x 3 x 1 for visualisation



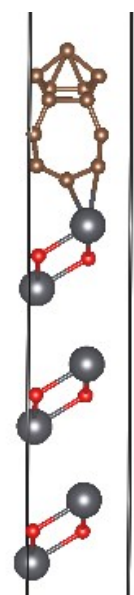
Initial carbon binding model to  $\alpha$ -PbO(001) 5L



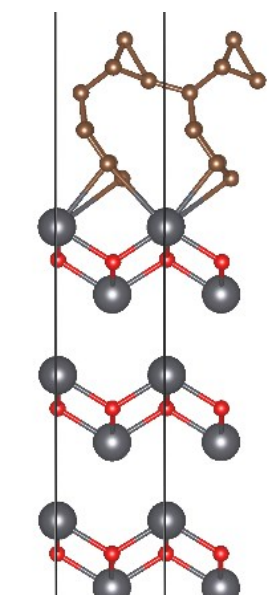
Initial binding to  $\alpha$ -PbO(001) 5L  
2 x 1 x 1 for visualisation



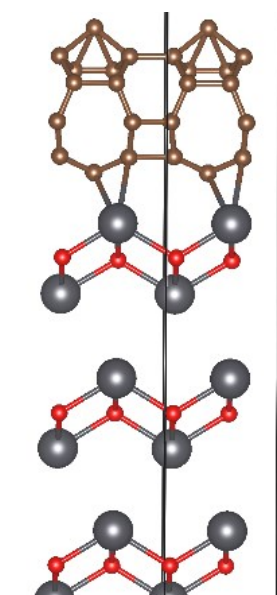
Initial binding to  $\alpha$ -PbO(001) 5L  
1 x 2 x 1 for visualisation



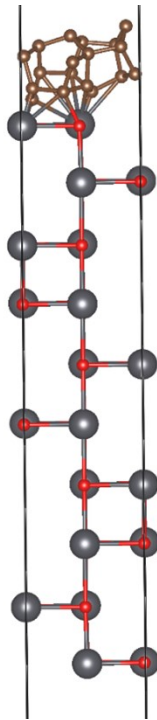
Optimised carbon binding model to  $\alpha$ -PbO(001) 5L



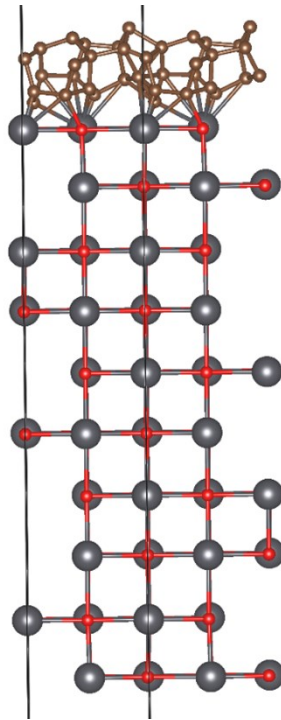
Optimised binding to  $\alpha$ -PbO(001) 5L  
2 x 1 x 1 for visualisation



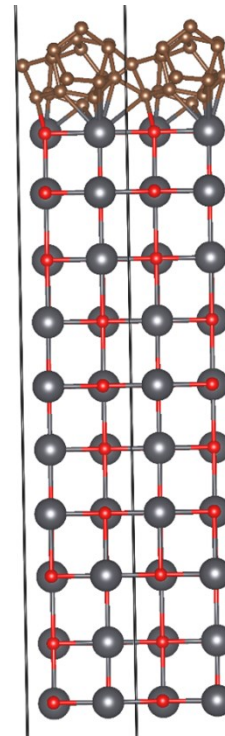
Optimised binding to  $\alpha$ -PbO(001) 5L  
1 x 2 x 1 for visualisation



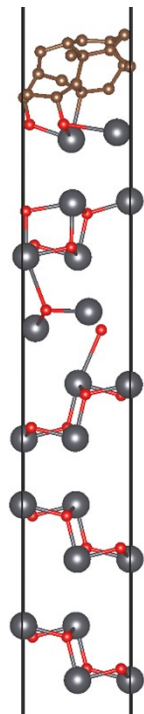
Initial carbon binding model to  $\beta$ -PbO(100) 5L



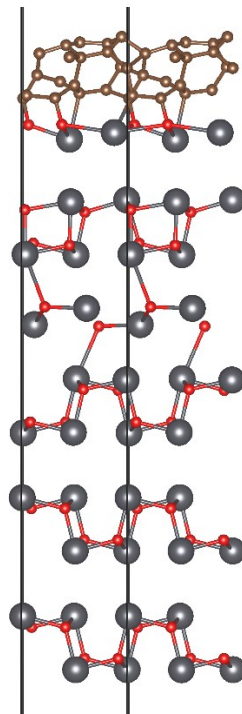
Initial binding model to  $\beta$ -PbO(100) 5L  
1 x 2 x 1 for visualisation



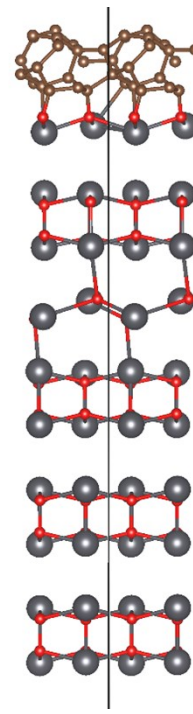
Initial binding to  $\beta$ -PbO(100) 5L  
1 x 1 x 2 for visualisation



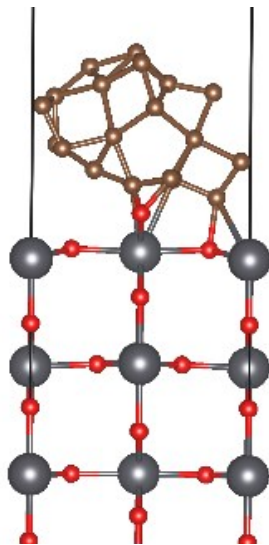
Optimised carbon binding model to  $\beta$ -PbO(100) 5L



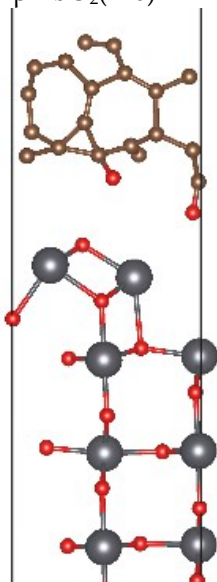
Optimised binding model to  $\beta$ -PbO(100) 5L  
1 x 2 x 1 for visualisation



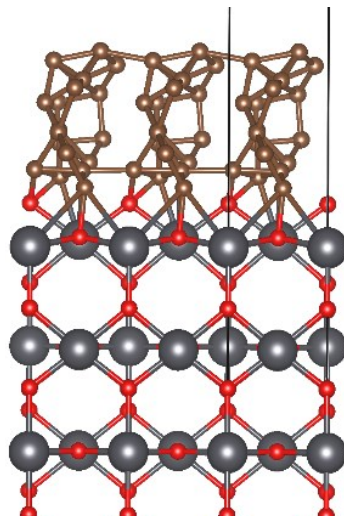
Optimised binding model to  $\beta$ -PbO(100) 5L  
1 x 1 x 2 for visualisation



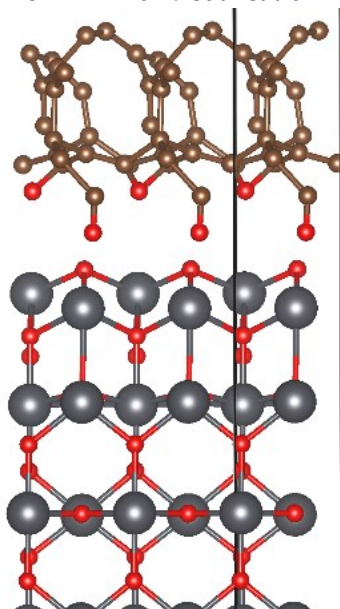
Initial carbon binding model to  $\beta\text{-PbO}_2(110)$  7L



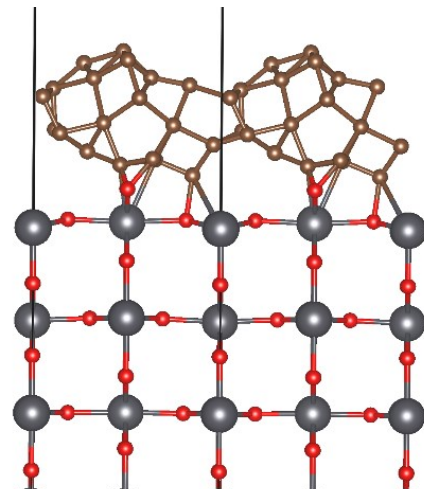
Optimised carbon binding model to  $\beta\text{-PbO}_2(110)$  7L



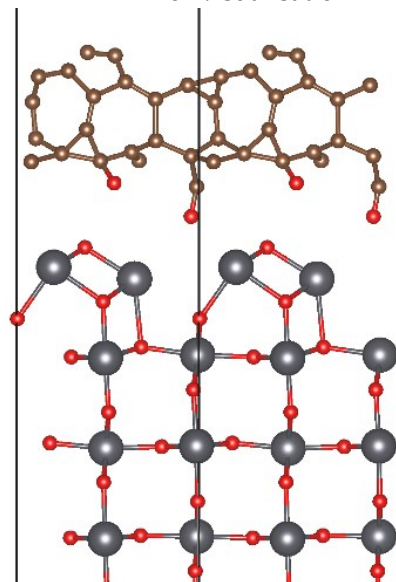
Initial binding to  $\beta\text{-PbO}_2(110)$  7L  
3 x 1 x 1 for visualisation



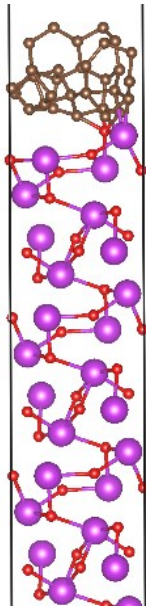
Optimised binding to  $\beta\text{-PbO}_2(110)$  7L  
3 x 1 x 1 for visualisation



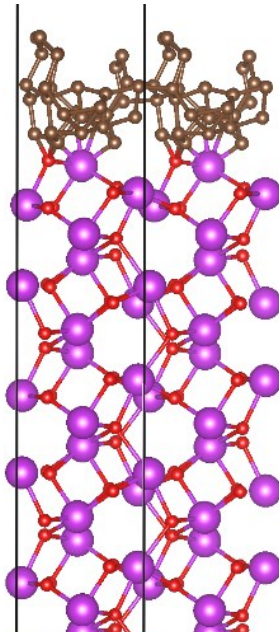
Initial binding to  $\beta\text{-PbO}_2(110)$  7L  
1 x 2 x 1 for visualisation



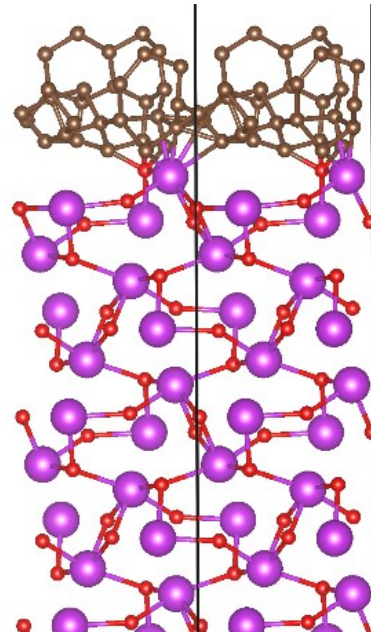
Optimised binding to  $\beta\text{-PbO}_2(110)$  7L  
1 x 2 x 1 for visualisation



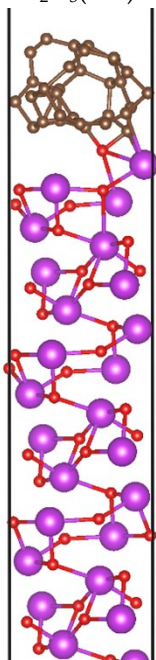
Initial carbon binding model to  $\alpha$ - $\text{Bi}_2\text{O}_3(010)$  5L



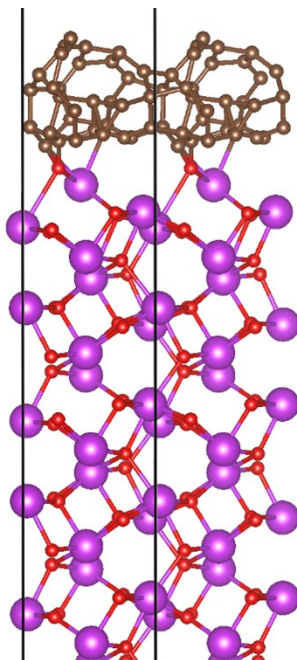
Initial binding to  $\alpha$ - $\text{Bi}_2\text{O}_3(010)$  5L  
2 x 1 x 1 for visualisation



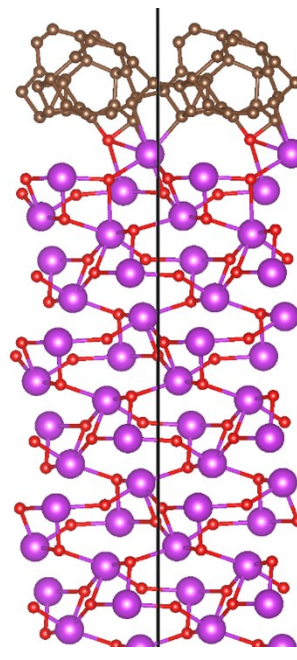
Initial binding to  $\alpha$ - $\text{Bi}_2\text{O}_3(010)$  5L  
1 x 1 x 2 for visualisation



Optimised carbon binding model to  $\alpha$ - $\text{Bi}_2\text{O}_3(010)$  5L



Optimised binding to  $\alpha$ - $\text{Bi}_2\text{O}_3(010)$  5L  
2 x 1 x 1 for visualisation



Optimised binding to  $\alpha$ - $\text{Bi}_2\text{O}_3(010)$  5L  
1 x 1 x 2 for visualisation

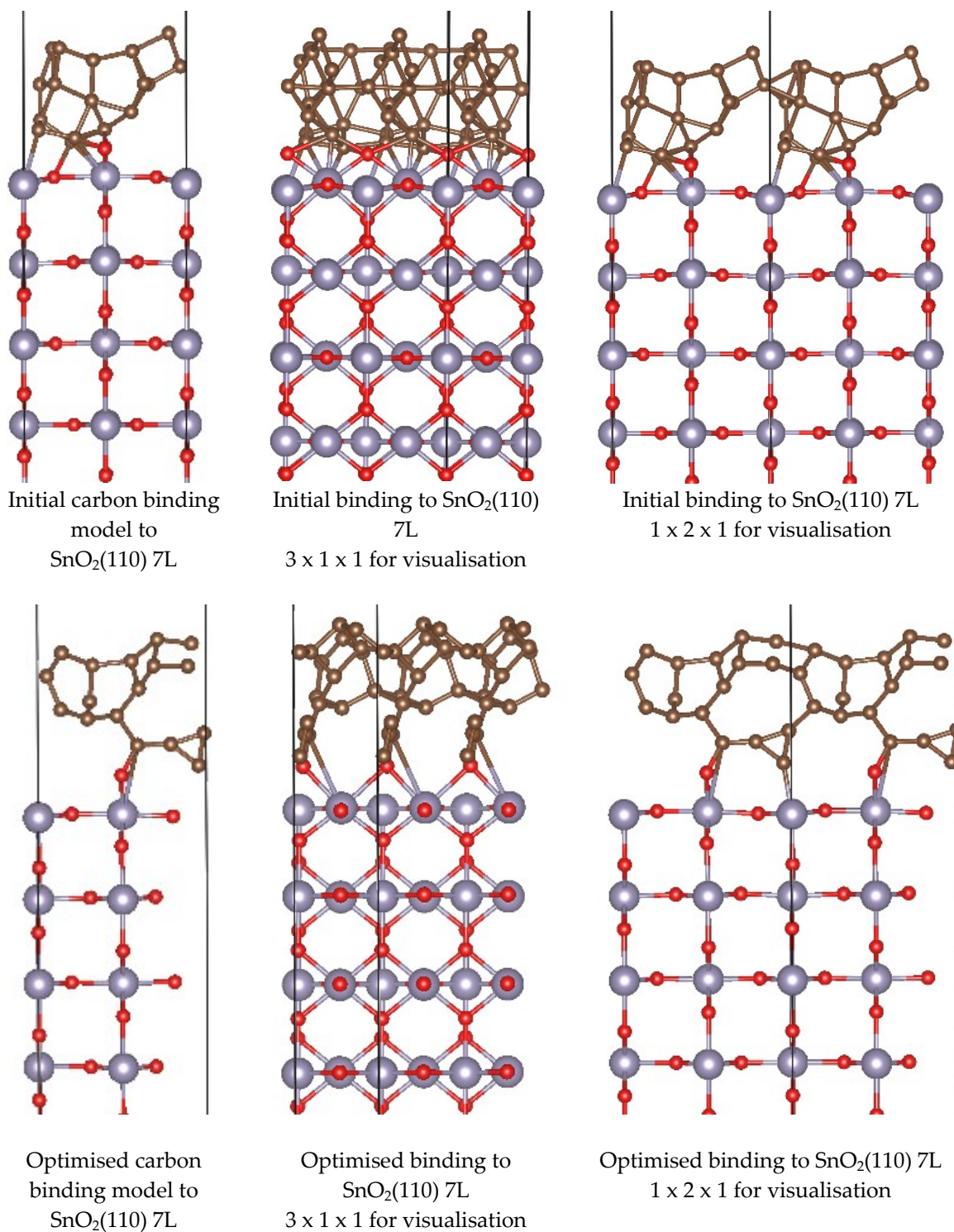


**Figure S4.** Initial (top) and optimised (bottom) adsorption models for binding amorphous carbon to each surface for Pb (111),  $\alpha$ -PbO (001),  $\beta$ -PbO<sub>2</sub> (110), SnO<sub>2</sub> (110) and  $\alpha$ -Bi<sub>2</sub>O<sub>3</sub> (010).

**Table S2.** Carbon binding data for ballistic modifier surfaces, including binding energies and optimised bond lengths. The 's' subscript indicates a surface atom. Binding energies computed with PBE-TS functional.

System	Pb (111)	$\alpha$ -PbO (001)	$\beta$ -PbO (100)	$\beta$ -PbO <sub>2</sub> (110)	$\alpha$ -Bi <sub>2</sub> O <sub>3</sub> (010)	SnO <sub>2</sub> (110)
Carbon binding energy (eV/ Å <sup>2</sup> )	-0.09	-0.06	Surface destroyed	Surface destroyed	-0.18	-0.29
Shortest M <sub>s</sub> -C bond length (Å)	3.83	2.49	2.44	4.12	2.46	2.12/ 3.15
Shortest O <sub>s</sub> -C bond length (Å)	-	3.56	1.42/1.44	1.20 / 1.38 / 3.70	1.46 / 3.50	1.39/ 2.83

## References

- 1 B. K. Meyer, A. Polity, D. Reppin, M. Becker, P. Hering, P. J. Klar, T. Sander, C. Reindl, J. Benz, M. Eickhoff, C. Heiliger, M. Heinemann, J. Blasing, A. Krost, S. Shokovets, C. Muller and C. Ronning, *Phys. Status Solidi*, 2012, **249**, 1487–1509.
- 2 S. C. Ray, *Sol. Energy Mater. Sol. Cells*, 2001, **68**, 307–312.
- 3 K. I. Hardee and A. J. Bard, *J. Electrochem. Soc.*, 1977, **124**, 215–224.
- 4 F. P. Koffyberg and F. A. Benko, *J. Appl. Phys.*, 1982, **53**, 1173.
- 5 F. Marabelli, G. B. Parravicini and F. Salghetti-Drioli, *Phys. Rev. B*, 1995, **52**, 1433.
- 6 T. P. Debies and J. W. Rabalais, *Chem. Phys.*, 1977, **20**, 277–283.
- 7 H. Cheng, B. Huang, J. Lu, Z. Wang, B. Xu, X. Qin, X. Zhang and Y. Dai, *Phys. Chem. Chem. Phys.*, 2010, **12**, 15468–15475.